Phytochemistry 146 (2018) 8–15

Contents lists available at ScienceDirect

Phytochemistry

journal homepage: www.elsevier.com/locate/phytochem

Anti-inflammatory meroterpenoids from the mangrove endophytic fungus *Talaromyces amestolkiae* YX1

Senhua Chen [a, 1], Meng Ding [a, 1], Weiyang Liu [c], Xishan Huang [a, *], Zhaoming Liu [a], Yongjun Lu [b], Hongju Liu [a, c, **], Zhigang She [a, ***]

[a] School of Chemistry, Sun Yat-Sen University, Guangzhou 510275, China
[b] School of Life Sciences and Biomedical Center, Sun Yat-Sen University, Guangzhou 510275, China
[c] School of Pharmacy, Guangdong Medical University, Dongguan, 523808, China

ARTICLE INFO

Article history:
Received 21 June 2017
Received in revised form
3 November 2017
Accepted 22 November 2017

Keywords:
Talaromyces amestolkiae
Trichocomaceae
Meroterpenoids
Mangrove endophytic fungus
Anti-inflammatory activity

ABSTRACT

Four previously undescribed meroterpenoids, amestolkolides A–D, along with three known compounds were isolated from the mangrove endophytic fungus *Talaromyces amestolkiae* YX1 cultured on wheat solid-substrate medium culture. Their structures were elucidated by a combination of spectroscopic analyses. The absolute configurations of amestolkolides B and C, and purpurogenolide E were determined by single-crystal X-ray diffraction using Cu Kα radiation, and those of amestolkolides A and D were elucidated on the basis of experimental and calculated electronic circular dichroism spectra. The absolute configuration of amestolkolides A-D, and purpurogenolide E (9*R*) at C-9 was different from that of analogues (9*S*) in references, so that their plausible and distinct biosynthetic pathways were proposed. Amestolkolide B showed strong anti-inflammatory activity *in vitro* by inhibiting nitric oxide (NO) production in lipopolysaccharide activated in RAW264.7 cells with IC_{50} value of 1.6 ± 0.1 μM.

1. Introduction

Meroterpenoids were hybrid natural products partially derived from mevalonic acid pathways and widely derived from animals, plants, bacteria, and fungi (Geris and Simpson, 2009; Matsuda and Abe, 2015). The meroterpenoids with the source of fungi exhibited diverse structural features and a wide range of biological activities, such as asperterpenes A and B with promising inhibitory activities against BACE1 (Qi et al., 2016), austalides with strong inhibition of *endo*-1,3-β-D-glucanase (Zhuravleva et al., 2014), mycophenolic acid as a strong inhibitor of inosine 5′-monophosphate dehydrogenase (IMPDH) (Sintchak et al., 1996), territrem B as a potent inhibitor of acetylcholinesterase (AChE) (Peng, 1995), berkeleyacetal C exhibited promising anti-inflammatory activity (Etoh et al., 2013). Among them, berkeleyacetals are the polyketide-terpenoid hybrid meroterpenoid class, possessing a unique and congested polycyclic skeleton with 6/7/6/5/6 system. Since paraherquonin was isolated from *Penicillium paraherquei* in 1983 (Okuyama et al., 1983), about 13 analogues, berkeleyacetals A–C (Stierle et al., 2007), miniolutelides A–B (Iida et al., 2008), 4,25-dehydrominiolutelide B, 4,25-dehydro-22-deoxyminiolutelide B, isominiolutelide A (Zhang et al., 2012), and purpurogenolides A–E (Sun et al., 2016) have been discovered mainly several fungi in the genus *Penicillium* (Li et al., 2014).

The genus *Talaromyces* was widespread around plants, foods, soil, as well as sponges (Zhai et al., 2016). The fungus could produce a wide range of secondary metabolites, such as anthraquinones (Bara et al., 2013), prenylated indole alkaloids (Chu et al., 2010), norsesquiterpene peroxides (Li et al., 2011), sesquiterpene lactones (Ngokpol et al., 2015), and meroterpenoids (Kaur et al., 2016).

Endophytic fungi have been demonstrated to be an important source of pharmacologically active metabolites (Debbab et al., 2013). In the last decade, our research group has focused on the mangrove endophytic fungi isolated from the South China Sea to discover novel and bioactive compounds (Chen et al., 2016a, 2016b, 2017a, 2017b; Li et al., 2011; Liu et al., 2016; Tan et al., 2016; Xiao et al., 2013). *Talaromyces amestolkiae* YX1 was cultured on solid wheat medium, which led to obtain four previously undescribed

* Corresponding author.
** Corresponding author. School of Chemistry, Sun Yat-Sen University, Guangzhou 510275, China.
*** Corresponding author.
E-mail addresses: huangxishan13@foxmail.com (X. Huang), liuhj8@mail2.sysu.edu.cn (H. Liu), cesshzhg@mail.sysu.edu.cn (Z. She).
[1] S.C. and M.D. contributed equally.

https://doi.org/10.1016/j.phytochem.2017.11.011
0031-9422/

meroterpenoids, amestolkolides A–D (**1**–**4**), along with three known compounds **5**–**7** (Fig. 1). Amestolkolides A and B (**1** and **2**) exhibited anti-inflammatory activity *in vitro* by inhibiting nitric oxide (NO) production in lipopolysaccharide activated in RAW264.7 cells with IC_{50} values of 30 ± 1.2 and 1.6 ± 0.1 μM, respectively. The isolation, structure elucidation, plausible biosynthetic pathways, and bioactivities of the isolates from the fungus are described herein.

2. Results and discussion

The mangrove endophytic fungus *Talaromyces amestolkiae* YX1 were cultured on solid wheat medium with artificial seawater for 28 days, respectively. The EtOAc extract of the wheat fermentation was fractionated by repeated silica gel chromatography and Sephadex LH-20 column chromatography to afford four previously undescribed meroterpenoids, amestolkolides A–D (**1**–**4**), together with three known meroterpenoids, purpurogenolide E (**5**) (Sun et al., 2016), chrodrimanin B (**6**) (Wei et al., 2011), and chrodrimanin A (**7**) (Hayashi et al., 2012).

Amestolkolide A (**1**) was obtained as white powder. The molecular formula was deduced to be $C_{24}H_{26}O_7$ on the basis of positive-ion HRESIMS (*m/z* 427.1746 $[M + H]^+$, calcd for $C_{24}H_{27}O_7$, 427.1751), implying 12 degrees of unsaturation. The IR spectrum indicated the presence of carbonyl (1778 and 1712 cm^{-1}) and olefinic (1612 cm^{-1}) functional groups. The ^1H NMR spectrum showed resonances for two olefinic protons [δ_H 6.02 (d, J = 1.5 Hz, H-2) and 6.14 (dd, J = 2.6, 1.5 Hz, H-14)], three oxygenated methines [δ_H 4.44 (dq, J = 6.7, 2.4 Hz, H-9), 4.97 (d, J = 2.6 Hz, H-13), and 6.01 (d, J = 4.5 Hz, H-22)], two methines [δ_H 2.56 (dd, J = 12.2, 4.3 Hz, H-5) and 2.91 (dd, J = 4.5, 2.5 Hz, H-21)], one oxygenated methylene [δ_H 3.14 (d, J = 5.5 Hz, H-24); 2.42 (d, J = 5.5 Hz, H-24)], one methylene [δ_H 1.70 (dd, J = 14.7, 4.3 Hz, H-6); δ_H 1.62 (dd, J = 14.7, 12.2 Hz, H-6)], five methyls [δ_H 1.47 (s, H-17), 1.66 (s, H-18), 1.31 (s, H-19), 1.36 (d, J = 6.7 Hz, H-20), and 1.30 (s, H-23)] (Table 1). The ^{13}C NMR spectrum (Table 1) revealed the presence of 24 carbons corresponding to two ester carbonyl groups (δ_C 163.4, 177.7), one ketal (δ_C 97.9), three double bonds (δ_C 105.2, 115.7, 128.1, 133.4, 150.4, 155.2), five methyls, two methylenes, five methines, one oxygenated tertiary carbon (δ_C 82.8), and two quaternary carbons (Table 1). These 1D NMR data (Table 1) with the help of the molecular formula suggested that **1** belonged to a heptacyclic meroterpenoid containing a hemiketal, three double bonds.

Analysis of the ^1H-^1H COSY spectrum suggested the presence of four isolated proton spin systems, CH(5)–CH_2(6), CH(9)–CH_3(20), CH(13)–CH(14), and CH(21)–CH(22) (Fig. 2). Key HMBC correlations from H-17 to C-16 and C-18, H-18 to C-15, and H-2 to C-1, C-3 and C-15 established a hexatomic ring lactone fragment (A ring) (Fig. 2). The HMBC correlations of H-5 with C-4, H-19 with C-5, C-12 and C-13, H-14 with C-3, H-13 with C-15 indicated a heptatomic ring fragment (B ring). The three rings system (C/D/E) was assigned by the correlations of H-6 to C-12 and C-21, H-23 to C-6, C-7, and C-8, H-21 to C-8, H-22 to C-8, C-9, and C-11, as well as H-20 to C-9 and C-10. The oxirane moiety was located at C-4, which was supported by the HMBC correlations of H-24 with C-4 and C-3, as well as the chemical shifts of C-4 (δ_C 58.0) and C-24 (δ_C 55.8). An ether linkage between C-10 and C-13 was fused as a furan unit according to the chemical shifts of C-10 (δ_C 150.4) and C-13 (δ_C 90.5), as well as the required degrees of unsaturation.

Table 1
^1H (500 MHz) and ^{13}C (125 MHz) NMR data for compounds **1**–**2** in $CDCl_3$.

no.	**1**		**2**	
	δ_C, type	δ_H, (J in Hz)	δ_C, type	δ_H, (J in Hz)
1	163.4, C		162.5, C	
2	115.7, CH	6.02, d, (1.5)	117.8, CH	6.11, d, (1.5)
3	155.2, C		152.2, C	
4	58.0, C		59.4, C	
5	37.5, CH	2.56, dd, (12.2, 4.3)	32.4, CH	3.02, dd, (12.8, 4.9)
6	27.6, CH_2	1.70, dd, (14.7, 4.3)	27.5, CH_2	2.02, dd, (14.7, 4.9)
		1.62, dd, (14.7, 12.2)		1.51, dd, (14.6, 12.9)
7	46.6, C		43.4, C	
8	177.7, C		176.1, C	
9	63.6, CH	4.44, dq, (6.7, 2.4)	74.3, CH	4.27, q, (7.1)
10	150.4, C		211.7, C	
11	105.2, C		51.7, CH	3.66, d, (9.9)
12	47.7, C		48.1, C	
13	90.5, CH	4.97, d, (2.6)	204.9, C	
14	128.1, CH	6.14, dd, (2.6, 1.5)	130.1, CH	6.34, d, (1.5)
15	133.4, C		141.8, C	
16	82.8, C		82.9, C	
17	26.2, CH_3	1.47, s	26.8, CH_3	1.61, s
18	25.8, CH_3	1.66, s	26.4, CH_3	1.67, s
19	19.5, CH_3	1.31, s	17.6, CH_3	1.17, s
20	17.7, CH_3	1.36, d, (6.7)	17.2, CH_3	1.32, d, (7.1)
21	40.9, CH	2.91, dd, (2.5, 4.5)	46.0, CH	3.15, dd, (9.9, 5.4)
22	97.9, CH	6.01, d, (4.5)	98.8, CH	6.14, d, (5.4)
23	24.2, CH_3	1.30, s	27.0, CH_3	1.34, s
24	55.8, CH_2	3.14, d, (5.5)	55.1, CH_2	3.19, d, (5.0)
		2.42, d, (5.5)		2.63, d, (5.0)

The relative configuration of **1** was determined on the basis of NOESY data (Fig. 3). NOE interactions H-21 with H-19, H-22, and H-23, H-22 with H-20 and H-23, H-13 with H-19 indicated their cofacial orientation. Furthermore, the correlations of H-5 with H-24 suggested that these protons were located on the opposite face (Fig. 3). The absolute configuration of **1** was assigned by comparison of the experimental and theoretical ECD spectra, which was calculated by a quantum chemical method at the [B3LYP/6-311+g(2d,p)] level. The predicted ECD spectrum of 4*R*, 5*R*, 7*R*, 9*R*, 12*S*, 13*S*, 21*S*, and 22*R* was in good agreement with that of the experimental one (Fig. 4). Thus, compound **1** was established as (1*R*,2a*R*,2a1*S*,4a*R*,5a*R*,5a1*S*,6*R*,11a*S*)-1,4a,5a1,10,10-pentamethyl-2a,2a1,4a,5,5a,5a1,10,11a-octahydro-8*H*-2,3,9,12-tetraoxaspiro

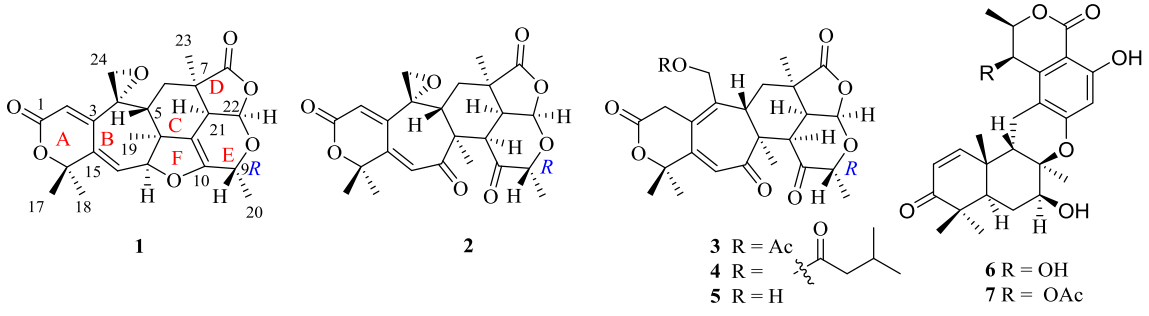

Fig. 1. Chemical structures of **1**–**7**.